

# Demonstration of an ultra-wideband optical fiber inline polarizer with metal nano-grid on the fiber tip

Yongbin Lin<sup>1\*</sup>, Junpeng Guo<sup>1,2</sup> and Robert G. Lindquist<sup>1,2</sup>

<sup>1</sup>Nano and Micro Device Center, University of Alabama in Huntsville, Huntsville, Alabama 35899

<sup>2</sup>Department of Electrical and Computer Engineering, University of Alabama in Huntsville, Huntsville, Alabama 35899

\*Liny@email.uah.edu

**Abstract:** Dramatic increase in the bandwidth of optical fiber inline polarizer can be achieved by using metal nano-grid on the fiber tip. However, high extinction ratio of such fiber polarizer requires high spatial frequency metal nano grids with high aspect ratio on the small area of optical fiber tip. We report the development of a nano-fabrication process on the optical fiber tip, and the design and realization of the first ultra-wideband fiber inline polarization device with Au nano grid fabricated on a single mode optical fiber end face.

©2009 Optical Society of America

**OCIS codes:** (060.2340) Fiber optics components; (260.5430) Polarization; (220.4241) Nanostructure fabrication

---

## References and links

1. H. Sunnerud, M. Karlsson, C. Xie, and P. A. Andrekson, "Polarization-mode dispersion in high-speed fiber-optic transmission systems," *J. Lightwave Technol.* **20**(12), (2002).
2. D. C. Cullen, R. G. Brown, and C. R. Lowe, "Detection of immuno-complex formation via surface plasmon resonance on gold-coated diffraction gratings," *Biosensors* **3**(4), 211–225 (1987-1988-1988).
3. M. Piliarik, J. Homola, Z. Manikova, and J. Ctyroky, "Surface plasmon resonance sensor based on a single-mode polarization-maintaining optical fiber," *Sens. Actuators B Chem.* **90**(1-3), 236–242 (2003).
4. H. C. Su, and L. A. Wang, "A highly efficient polarized superfluorescent fiber source for fiber-optic gyroscope applications," *IEEE Photon. Technol. Lett.* **15**(10), 1357–1359 (2003).
5. R. A. Bergh, H. C. Lefevre, and H. J. Shaw, "Single-mode fiber-optic polarizer," *Opt. Lett.* **5**(11), 479 (1980).
6. J. R. Feth, and C. L. Chang, "Metal-clad fiber-optic cutoff polarizer," *Opt. Lett.* **11**(6), 386–388 (1986).
7. W. Johnstone, G. Stewart, T. Hart, and B. Culshaw, "Surface plasmon polaritons in thin metal films and their role in fiber optic polarizing devices," *J. Lightwave Technol.* **8**(4), 538–544 (1990).
8. M. N. Zervas, and I. P. Giles, "Optical fiber surface plasmon wave polarizers with enhanced performance," *Electron. Lett.* **25**(5), 321 (1989).
9. A. Wang, V. Arya, M. H. Nasta, K. A. Murphy, and R. O. Claus, "Optical fiber polarizer based on highly birefringent single-mode fiber," *Opt. Lett.* **20**(3), 279–281 (1995).
10. G. R. Bird, and M. Parrish, Jr., "The wire grid as a near-infrared polarizer," *J. Opt. Soc. Am.* **50**(9), 886–891 (1960).
11. A. Petrušis, J. H. Rector, K. Smith, S. de Man, and D. Iannuzzi, "The align-and-shine technique for series production of photolithography patterns on optical fibers," *J. Micromech. Microeng.* **19**(4), 047001 (2009).
12. E. J. Smythe, M. D. Dickey, J. Bao, G. M. Whitesides, and F. Capasso, "Optical antenna arrays on a fiber facet for in situ surface-enhanced Raman scattering detection," *Nano Lett.* **9**(3), 1132–1138 (2009).
13. H. Sotobayashi, J. T. Gopinath, H. M. Shen, J. W. Sickler, P. T. Rakich, and E. P. Ippen, "Supercontinuum generation and its applications," *Proc. SPIE* **6014**, 60140T (2005), doi:10.1117/12.633412.
14. <http://www.nktp Photonics.com/side5228.html>
15. H. Wang, M. W. Jenkins, and A. M. Rollins, "A combined multiple-SLED broadband light source at 1300 nm for high resolution optical coherence tomography," *Opt. Commun.* **281**(7), 1896–1900 (2008).
16. A. D. Rakic, A. B. Djurišić, J. M. Elazar, and M. L. Majewski, "Optical properties of metallic films for vertical-cavity optoelectronic devices," *Appl. Opt.* **37**(22), 5271–5283 (1998).

---

## 1. Introduction

Optical fiber polarizer is desirable for discrimination between orthogonal linear polarization states of light propagating in the optical fiber. It has important applications ranging from optical transmission system to chemical and biological optical fiber sensors and fiber-optic

gyroscope [1–4]. Based on their fundamental constructions, optical fiber polarizer can be divided into two types. One is fiber polarizer constructed from bulk free space optics, which suffers from high loss, high cost, difficult to package and particularly, mechanical instability. The other one is fiber inline polarizer, which is more desirable for low loss and simpler to package.

The first single-mode fiber inline polarizer was developed in 1980 [5] by Bergh and colleagues. In this work part of the fiber cladding was removed and a birefringent crystal was placed close to fiber core. The property of different refractive index for two orthogonal linear polarization states was used to separate the transverse electric (TE) wave and transverse magnetic (TM) wave. In order to overcome large volume from birefringent crystal, two technologies for realizing fiber inline polarizer had been brought forward. One is based on the TM-only nature of surface plasmon resonance (SPR) for polarization selectivity [6–8]. The other one is based on periodic perturbation on optical fiber generated by micro-bends, acoustic wave, photorefractive index grating or twisting. This type of design makes use of the characteristics of fiber grating different mode coupling due to fiber core birefringent property [9].

High spatial frequency metal wire grids has long been recognized as an effective method for optical polarizer for a very broad wavelength range [10]. In this paper we propose to design and fabricate the high spatial frequency nano-grids on the optical fiber tip to realize ultra-wideband fiber inline polarizer. Unlike the SPR based or periodic perturbation based fiber inline polarizer, whose operational bandwidth is fundamentally limited by phase matching condition, the metal nano-grid based polarizer does not have the phase-matching constrain, therefore it is possible to realize ultra-wideband optical fiber polarizer. However, to our knowledge, there is no literature report on the realization of such device.

Patterning and nano fabrication process on the optical fiber tip has draw lots of researcher's attention recently. Various fabrication techniques had been reported [11, 12]. In this paper we present our approach based on electron beam lithography (EBL) and reactive-ion etching (RIE) that allows rapid prototypes of nano and micro structures on optical fiber tip.

There are a growing demand for wideband, high extinction ratio and low loss fiber polarization components, especially with the recent emerging technologies for ultra-broadband light source in optical fiber, such as supercontinuum light source [13, 14] and superluminescent light emitting diode (SLED) [15]. These broadband light sources featured very wide bandwidth, high optical power output, and randomly oriented polarization state. For example, the bandwidth for the fiber pigtailed supercontinuum light source covers 500nm to 2400nm [14]. An ultra-wideband and high extinction ratio fiber polarizer is desirable for these broadband fiber light source. Unfortunately, current optical fiber inline polarizer cannot meet the bandwidth requirement for these wideband fiber light sources.

In response to this need, we present in this paper a detailed design and fabrication process to realize ultra-wideband optical fiber inline polarizer with high spatial frequency metal nano-grid on the optical fiber tip. Transmission characterizations of the fabricated device are also presented, along with discussions and conclusions.

## 2. Design

The nano-grid polarizer on the optical fiber tip under consideration is illustrated in Fig. 1. The optical properties of the nano-grid polarizer are depended on parameters such as complex refractive index of the metal, the period of the nano-grid ( $\Lambda$ ), the thickness of the wire ( $d$ ) and the fill factor ( $f$ ), which is defined as the ratio of the width of a single wire to the period of the nano-grid. In order to achieve high extinction ratio in the infrared (IR) and visible region, the nano-grid polarizers are required to have a high spatial frequency with large aspect ratio.

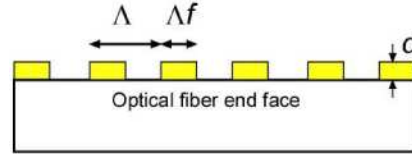


Fig. 1. Nano-grid polarizer with Au grating on the optical fiber tip.

We use rigorous coupled-wave analysis theory (RCWA) for the numerical analysis of the performance of the fiber tip Au nano-grid polarizer. For simplicity, the incident monochromatic plane wave is used instead of fiber mode wave in the numerical analysis. The Lorentz-Drude model was used for the complex electric permittivity of Au at visible and IR wavelengths [16].

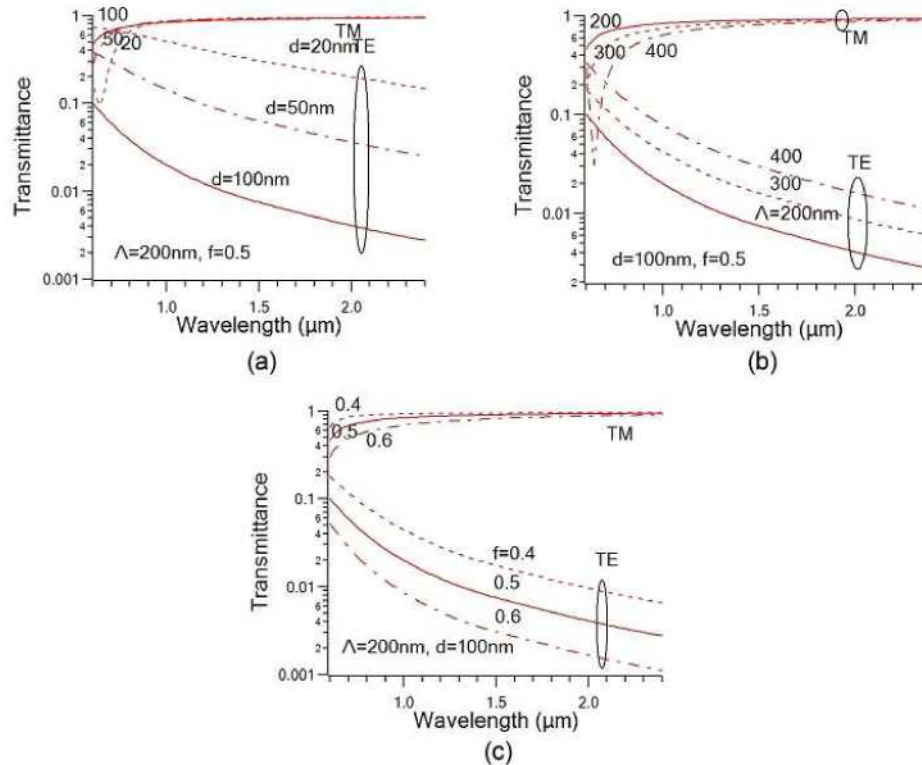


Fig. 2. Simulation results for transmission spectra of Au nano-grid polarizer when (a) Au nano-grid thickness is varied while grating period and fill factor are assumed as 200nm and 0.5. (b) Grating period is varied while Au nano-grid thickness and fill factor are assumed as 100nm and 0.5. (c) The filled factor is varied while Au nano-grid thickness and period are assumed as 100nm and 200nm.

Figure 2(a) shows the transmission spectra as a function of wavelength for three different nano-grid thickness ( $d=20\text{nm}$ ,  $50\text{nm}$  and  $100\text{nm}$ ). The nano-grid period is assumed to be  $200\text{nm}$  and the fill factor is assumed to be  $0.5$ . As indicated in Fig. 2(a), the TE transmission decreases with the increase of the nano-grid thickness, while the TM transmission is almost constant. A higher extinction ratio can be achieved with large nano-grid thickness, which in turn is determined in micro-fabrication by the maximum achievable wire aspect ratio whether the wires are formed with an etch or a lift-off process.

Figure 2(b) shows the transmission spectra as a function of wavelength for the variation of the grating periods ( $\Lambda=200\text{nm}$ ,  $300\text{nm}$  and  $400\text{nm}$ ). The Au grating thickness is assumed to be  $100\text{nm}$  and the fill factor is assumed to be  $0.5$ . As indicated in Fig. 2(b), the TE

transmission decreases and TM transmission increases with the decrease of the grid period. A better extinction ratio and lower loss can be obtained with higher slit density. However, it is practically limited by the minimum feature size of the patterning tool used in the micro-fabrication process lab.

Figure 2(c) shows the transmission spectra as a function of wavelength for three different Au nano-grid fill factors ( $f=0.4, 0.5, 0.6$ ). Au nano-grid thickness and period are assumed as 100nm and 200nm. As portrayed in Fig. 2(c), while TE transmission decrease with the higher fill factor, the TM transmission decrease also. Designing a metal nano-grid fiber polarizer for a particular application involves careful trade-offs between the extinction ratio and optical throughput. In our initial fabrication development, we use a moderate fill factor ( $f=0.5$ ).

### 3. Device fabrication

We fabricated Au nano-grid polarizer on the end face of a standard optical fiber SMF-28, which has single mode operation for the wavelength of 1310nm. The overall fabrication process is illustrated in Fig. 3. The outer buffer coating on the optical fiber was removed using a stripper, and the fiber tip was cleaved perpendicularly to get a flat end face. 2 nm of Cr was deposited on the fiber tip by vacuum sputtering method as adhesive layer, followed by 100nm of gold film deposition in the same chamber. Electron beam (e-beam) resist ZEP 520A was coated on the fiber tip by a special dip and vibration coating technique described below. To get an optimized ZEP thickness, we diluted the ZEP 520A with solvent anisole at the ratio 1:1. Immediately after dipping in the diluted ZEP solution, the fiber tip was gently taken out, hold by a fiber clamp and put in the straight upward position. We use a method called “vibration coating” to get rid of extra liquid e-beam resist. The vibration frequency and strength is controlled by the length of fiber tip outside of the fiber clamp and the initial displacement of the fiber tip. After the dip and vibration coating, the fiber tip was baked in a 120°C oven for 30 minutes. The resulted ZEP film thickness was found to be around 80nm to 100nm by scanning electron microscope (SEM) observation. In order to minimize the charging effect in the EBL process, a layer of conductive polymer was coated on the fiber tip, using the same dip and vibration coating technique. Then the fiber tip was baked for 10 minutes in the 120°C oven. The EBL process was used to create the high spatial frequency grid pattern in the e-beam resist. The voltage used was 30kV and the dose was  $80\mu\text{C}/\text{cm}^2$ . After e-beam exposure, the conductive polymer was removed by DI water rinse for 1 minute. Pure nitrogen stream was used to dry the fiber tip. The fiber tip was developed by dipping in the e-beam resist developer (ZEP N50) for 1 minute, followed by DI water rinse for 1 minute. The sample was dried by a pure nitrogen stream and baked in the 120°C oven for 30 minutes for dehydration and hardening.

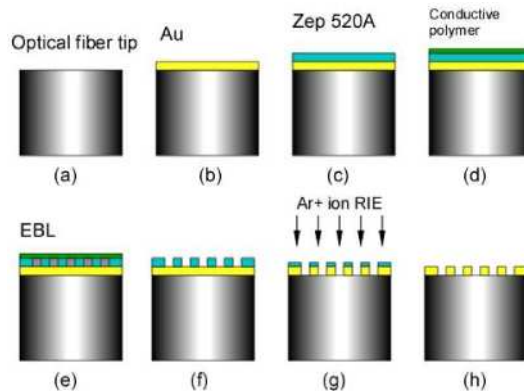


Fig. 3. Fabrication process of nano-grid polarizer with Au grating on the optical fiber tip.

The nano grid pattern in the e-beam resist was transferred to Au layer by RIE etch with Ar+ ion. The ZEP film prepared above was found not strong enough to stand for the high

surface temperature resulted from Ar<sup>+</sup> ion bombardment in the RIE etch. The ZEP film was found melted and reflow within 1 minute of RIE etch. However, we discovered that if we flood expose the ZEP film with electron beam at 5KV, the ZEP film will become stronger, and can stand for the high temperature in RIE etch process. The etch time was 7.5 minutes with 200W platen power and Ar gas flow rate of 20 sccm. The remaining ZEP film was striped by dip in the acetone for 1 minute.

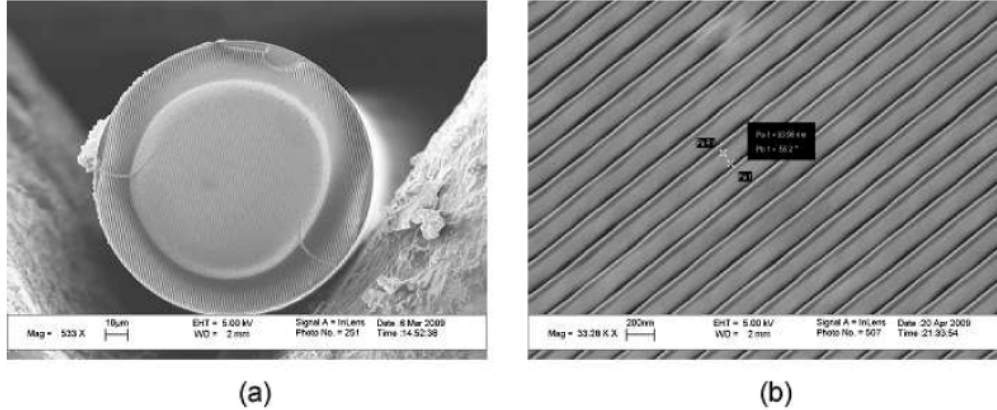


Fig. 4. Scanning electron micrograph of fiber tip nano-grid polarizer. (a) overview of the optical fiber end face, and (b) Au nano-grid with thickness  $d=100\text{nm}$ , period  $\Lambda=200\text{nm}$  and fill factor  $\sim 0.5$ .

The SEM image of the Au nano grid on optical fiber tip is shown in Fig. 4(a). The circle in the fiber tip is attributed to the e-beam resist film thickness variation due to edge bead. The ZEP film thickness inside of the circle is uniform. The diameter of the uniform thickness area is found to be around  $80\mu\text{m}$ , which is large enough to cover the fiber mode diameter ( $\sim 10\mu\text{m}$ ). Figure 4(b) shows the zoom in image of nano-grid at the center of the optical fiber tip.

#### 4. Device characterization

The transmittance of the fabricated optical fiber polarizer was measured by launching polarized diode laser light into the input fiber, which incorporated an all-fiber 3-paddle polarization controller. The input fiber is butt coupled to the nano-grid polarizer fiber tip using a Newport autoalign system for alignment. The output light intensity was measured by an optical power detector. No index matching fluid was used. The polarization controller was used to adjust the state of polarization at the device input, and the ratio of the minimum to maximum transmitted intensity was taken as the extinction ratio.

We measure the extinction ratio of the device at the wavelength of 850nm, 1310nm, 1480nm, 1550nm and 1580nm. Two diode lasers (850nm and 1310nm) and an Agilent tunable laser with wavelength range from 1480nm to 1580nm were involved in the measurement.

As shown in Fig. 5(a), the extinction ratio of the fabricated element is close to or higher than 20dB at wavelengths around 1.5 $\mu\text{m}$ , agree well with the simulation prediction. For 1310nm and 850nm wavelength, the extinction ratio is around 4dB lower than the prediction, which we think is caused partially by the lower polarization extinction ratio of the laser diodes used in the experiment. The insertion loss of the element, as shown in Fig. 5(b) shows around 2dB lower than the simulation prediction for wavelengths of 1310nm and longer, which is attributed to the fiber butt coupling loss, additional length of optical fiber and the device manufacture imperfection. The fiber butt coupling loss is typically in the range of 0.25 to 0.6 dB in our alignment system, measured by using dummy cleaved fiber tips. There is extra insertion loss for wavelength of 850nm, which could be attributed to the multimode propagation and coupling, since the wavelength is shorter than the fiber cutoff wavelength (1310nm) for single-mode operation. Future improvement for the device performances is

underway, which includes higher density of the Au nano-grid in the EBL patterning process, and improving RIE process to get a higher aspect ratio.

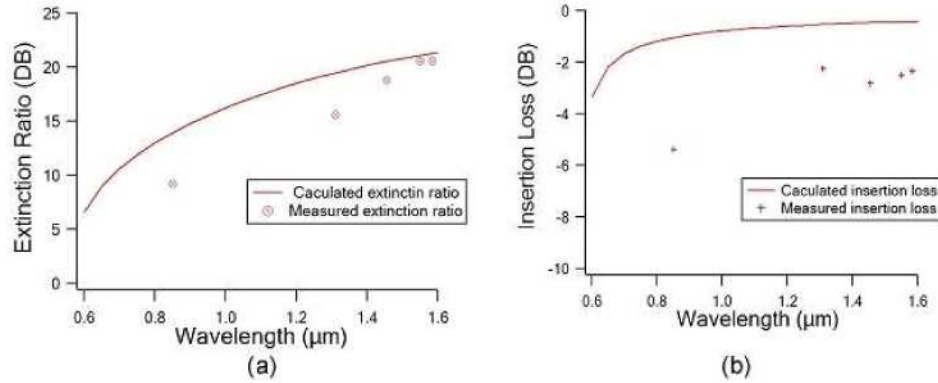


Fig. 5. (a) Measured extinction ratio of the fabricated element at different wavelengths. (b) The power throughput (insertion loss) of the element.

## 5. Conclusion

We have designed and fabricated a wideband optical fiber inline polarizer based on the high spatial frequency Au nano-grid on the fiber tip, and developed a fabrication process for the device realization. The fabricated element demonstrated 20.5dB extinction ratio at wavelength of 1550nm and 15.6dB at the wavelength of 1310nm. This device can work with the supercontinuum optical fiber broadband light source and SLED broadband optical fiber pigtailed broadband light source to yield a wideband polarized light in optical fiber, which has important applications in chemical and biological sensing.

## Acknowledgements

This work was supported by the NASA EPSCOR program under grant number NNX07AT55A, and NSF EPSCOR program under grant number SUB-2008-EPS-0814103-CIDEN-UAH.